Polymer Chemistry

Accepted Manuscript

ROYAL SOCIETY OF CHEMISTRY

www.rsc.org/polymers

Polymer Chemistry

Paper

Regio- and stereoselective construction of stimuli-responsive macromolecules by a sequential coupling-hydroamination polymerization route

Received 00th January 20xx,
Accepted 00th January 20xx

DOI: 10.1039/x0xx00000x

www.rsc.org/

Haiqin Deng,[ab] Zikai He,[ab] Jacky W. Y. Lam,*[ab] and Ben Zhong Tang*[abc]

Herein we reported a new facile one-pot multicomponent sequential polymerization approach for the construction of conjugated nitrogen-substituted polymers. Catalyzed by $Pd(PPh_3)_2Cl_2$/CuI at room temperature, the coupling-hydroamination polymerizations of 1,2-bis(4-ethynylphenyl)-1,2-diphenylethene, terephthaloyl chloride and secondary aliphatic amines proceeded smoothly in a regioregular and stereoselective manner, furnishing poly(arylene enaminone)s (PAEs) with high molecular weights (M_w up to 34 600) in satisfactory yields (up to 91%). Model compound was eleborately designed and synthesized to verify the chemical structures of the corresponding polymeric products. All the PAEs exhibited good solubility in common organic solvents and were thermally stable with degradation temperatures of up to 313 °C under nitrogen. They possessed good film-forming ability and their thin solid films showed high refractive indices (RI = 1.9318–1.6320) in a wide wavelength region of 400–1000 nm, whose value could be further modulated by UV irradiation. Although the model compound and the PAEs possessed a typical aggregation-induced emission luminogen of tetraphenylethene, they were weakly emissive either in solutioins or at the aggregated state, due to the photoinduced electron transfer (PET) effect. Their strong emission in the aggregated state could be readily recovered by blockage of the PET effect through protonation of the amino groups. Thus, this work demonstrated a powerful polymerization tool to access conjugated polymeric materials with pH-responsive properties.

Introduction

As a branch of tandem reactions[1], sequential reactions incorporate two or more distinct transformations into one single sequence, and are one of the most powerful synthetic methodologies for the rapid buildup of molecular complexity and diversity.[2] Different from the conventional stepwise synthetic protocols, which suffer from complex reaction procedures, harsh reaction conditions, painful isolations, severe side reactions, etc.,[3] sequential reactions enjoy unique atom economy, high efficiency, simple reaction and isolation procedures.[4] With these compelling advantages, sequential reactions have attracted much attention in promoting the elegance of synthesis and the development of green chemistry.[5] Particularly, chemists have made great endeavor to introduce the sequential reactions into polymer field in some reported frontier works.[6] Recently, catalytic sequential reactions involving hydroelement addition to alkyne have been widely investigated.[1] Among them, the palladium-catalyzed sequential reaction is one of the most efficient strategies for the construction of a variety of complicated molecular skeletons.[7] However, to date only limited palladium-catalyzed sequential reactions involving hydroelement additions to alkyne were explored for the construction of conjugated heteroatom-substituted polymers.[8]

Recently, a three-component coupling-hydrothiolation-cyclocondensation reaction of alkyne, aroyl chloride, and ethyl 2-mercaptoacetate was successfully developed into an efficient polymerization technique for preparing conjugated poly(arylene thiophenylene) by our group.[9] To extend the reaction scope, we intend to use amines to construct polymers via sequential coupling-hydroamination polymerization. However, polyhydroaminations with direct addition of amines to alkynes are rarely reported.[10] Actually, it is a great challenge to synthesize such conjugated nitrogen-substituted polymers with well-defined structures by using polyhydroaminations. As shown in Scheme 1A, the reaction of an alkyne with a primary amine generally gives a mixture of enamine stereoisomers, whose tautomerization generates their regioisomeric imine counterpairs. In 2003, Müller and his coworkers reported that the one-pot three-component sequential coupling-addition

[a] HKUST-Shenzhen Research Institute, No. 9 Yuexing 1st RD, South Area, Hi-tech Park, Nanshan, Shenzhen 518057, China. chjacky@ust.hk; tangbenz@ust.hk.
[b] Department of Chemistry, Institute for Advanced Study, Institute of Molecular Functional Materials, Division of Biomedical Engineering, Division of Life Science and State Key Laboratory of Molecular Neuroscience, The Hong Kong University of Science & Technology, Clear Water Bay, Kowloon, Hong Kong.
[c] Guangdong Innovative Research Team, SCUT-HKUST Joint Research Laboratory, State Key Laboratory of Luminescent Materials and Devices, South China University of Technology, Guangzhou 510640, China.

† Electronic Supplementary Information (ESI) available: Crystal data and structure refinement for model compound **4**; TGA thermogram of P**1**/**2**/**3**; emission spectra of **4** in THF/water mixtures; emission spectra of P**1**/**2**/**3a** in THF/water mixtures; emission spectra of P**1**/**2**/**3a** in THF/water mixtures acidified with 0.5 mM HCl solution. See DOI: 10.1039/x0xx00000x

reaction of alkynes, carbonyl chlorides and primary amines catalyzed by $Pd(PPh_3)_2Cl_2$/CuI could afford sole *Z*-enaminones with high efficiency and excellent regio- and stereoselectivity (Scheme 1B).[11] The carbonyl group in the intermediate ynone introduced polarization across the triple bond, which facilitated its regioselective hydroamination with primary amine. The six-membered ring formed by intramolecular hydrogen bond, on the other hand, helped to stabilize the *Z*-vinylene structure, avoiding tautomerization and *E*/*Z* isomerization and hence achieving high stereoselectivity. Therefore, addition of primary amine to ynone provides a perfect solution to solve the problems occurred in polyhydroamination. What is the consequence when using secondary amines? As shown in Scheme 1C, tautomerization of products is avoided when using secondary amines as reactants.[12] Meanwhile, enamines with a predominant *E* configuration are obtained. Because of such promising results together with our rich experience in polymer science,[13] such one-pot three-component coupling-hydroamination reaction is possible to be developed into an efficient and practical polymerization protocol towards novel conjugated nitrogen-substituted polymers.

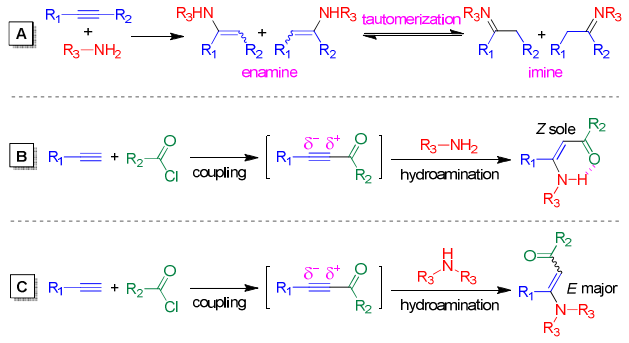

Scheme 1. (A) Alkyne hydroamination and enamine-imine tautomerization. (B and C) One-pot sequential coupling-hydroamination reactions of alkynes and carbonyl chlorides with (B) primary amines or (C) secondary amines.

In this work, we tried such possibility and herein showed that the polymerizations of tetraphenylethene (TPE)-containing diyne (**1**), terephthaloyl chloride (**2**) and secondary aliphatic amines (**3a** and **3b**) could proceed smoothly in THF under nitrogen in the presence of $Pd(PPh_3)_2Cl_2$, CuI and triethylamine (Et_3N) at room temperature, affording regioregular and stereoselective conjugated poly(arylene enaminone)s (P**1**/**2**/**3**) with high molecular weights in satisfactory yields. The resulting polymers displayed excellent solubility, good thermal stability, and high and tunable light refractivity. Although TPE was a well-known aggregation-induced emission (AIE) luminogen,[14] all the polymers were weakly emissive in both solution and aggregated state due to the photoinduced electron transfer (PET) effect. Their intense aggregated-state emission could be readily recovered by protonation. Such a change in the emission behavior in response to the variation in pH makes them potential environmentally sensitive macromolecules that can be crafted into new smart functional materials.[15]

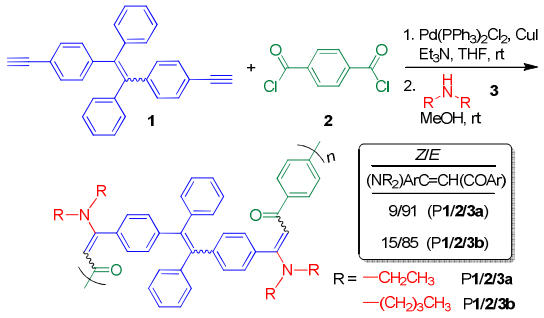

Scheme 2. Synthetic route to P**1**/**2**/**3** by three-component sequential polymerizations of diyne, diaroyl chloride and secondary amines.

Results and discussion

Polymerization

To exploit the organic reaction in Scheme 1C as a powerful tool for the buildup of functional conjugated polymers, we prepared diyne **1** according to our previous published work.[16] Monomer **2** and secondary amines (**3a** and **3b**), on the other hand, were commercially available. Diyne **1** was first reacted with **2** for 1 h at room temperature in THF under nitrogen in the presence of $Pd(PPh_3)_2Cl_2$, CuI and Et_3N. Afterwards, secondary amine **3a** or **3b** and methanol were injected into the reaction system to undergo the subsequent hydroamination reaction, producing nitrogen-containing conjugated poly(arylene enaminone)s (P**1**/**2**/**3**).

To search the best conditions for such polymerization, the effect of reaction time was first investigated using **1**, **2**, and **3a** as monomers (Table 1). Although the isolated yield slightly increased with prolonging the reaction time, the molecular weight of the polymeric products was significantly enhanced. The highest value (M_w = 34 600) was obtained at 30 h, whose value was 2.36-fold higher than that achieved at 12 h. This suggests the positive factor of the polymerization time to the polymerization process. Thus, we fixed 30 h as the optimized reaction time for the later investigation.

Table 1 Time course on the polymerization[a]

Entry	Yield (%)	Time (h)	M_w[b]	M_n[b]	M_w/M_n[b]
1	80	12	10 300	6 100	1.7
2	82	18	16 100	7 300	2.2
3	85	24	22 900	11 500	2.0
4	86	30	34 600	12 400	2.8

[a] Carried out in THF under nitrogen at room temperature in the presence of $Pd(PPh_3)_2Cl_2$, CuI and Et_3N. [Pd] = 4 mol%, [Cu] = 8 mol%, [Et_3N] = 0.10 M, [**1**] = 0.05 M, [**2**] = 0.05 M, [**3a**] = 0.15 M. Monomer **1** reacted with **2** for 1 h prior to the addition of **3a**. [b] Estimated by gel permeation chromatography (GPC) in THF on the basis of a linear polystyrene calibration.

We then studied the effect of monomer concentration on the polymerization while keeping the monomer feed ratio being constant. As shown in Table 2, when the polymerization was carried out at a relatively high monomer concentration of 0.10 M, insoluble gel was formed quantitatively before the addition of monomer **3a**. The obtained gel was also not soluble in other common organic solvents. Diluting the monomer

concentration to 0.05 M helped to suppress the gel formation and a soluble polymeric product with high M_w of 34 600 was, delightfully, isolated in 86% yield. When the concentration of monomer **1** was further decreased to 0.03 M or 0.02 M, soluble polymers with satisfactory molecular weights were also produced, albeit in reduced isolated yields.

Table 2 Effect of monomer concentration on the polymerization[a]

Entry	[**1**] (M)	Yield (%)	M_w[b]	M_n[b]	M_w/M_n[b]
1	0.10	gel			
2[c]	0.05	86	34 600	12 400	2.8
3	0.03	73	29 400	14 700	2.0
4	0.02	63	22 800	14 300	1.6

[a] Carried out in THF under nitrogen at room temperature for 30 h in the presence of $Pd(PPh_3)_2Cl_2$, CuI and Et_3N. [Pd] = 4 mol%, [Cu] = 8 mol%, [Et_3N] = 2[**1**]. [**2**] = [**1**], [**3a**] = 3[**1**], Monomer **1** reacted with **2** for 1 h prior to the addition of **3a**. [b] Estimated by GPC in THF on the basis of a linear polystyrene calibration. [c] Data taken from Table 1, entry 4.

We then studied the concentration effect of **3a** on the polymerization. As verified by the results shown in Table 3, the yield and the molecular weight of the obtained polymer decreased when a higher concentration of **3a** was used for the polymerization. The addition of more amine molecules to the intermediate poly(arylene ynonylene) chain furnishes a more steric bulky poly(arylene enaminone)s, which hampers its further growth by coupling reaction with **1** and **2**.

With these optimized reaction parameters in hand, we investigated the monomer scope for the polymerization. Similar to **3a**, polymerization employing dibutylamine (**3b**) also proceeded under mild conditions, affording soluble conjugated polymer P**1**/**2**/**3b** with high molecular weight (M_w = 32 100) in 91% yield (Table 4, entry 2). We also used diphenylamine or dibenzylamine for the polymerization but obtained no desired polymers, which demonstrated the important role of the steric bulkiness of the amine on the polymerization.

Table 3 Effect of amine concentration on the polymerization[a]

Entry	[**3a**] (M)	Yield (%)	M_w[b]	M_n[b]	M_w/M_n[b]
1[c]	0.15	86	34 600	12 400	2.8
2	0.20	81	27 100	12 900	2.1
3	0.25	81	17 900	9 900	1.8
4	0.30	64	15 500	8 600	1.8

[a] Carried out in THF under nitrogen at room temperature for 30 h in the presence of $Pd(PPh_3)_2Cl_2$, CuI and Et_3N. [Pd] = 4 mol%, [Cu] = 8 mol%, [Et_3N] = 0.1 M, [**1**] = 0.05 M, [**2**] = 0.05 M. Monomer **1** reacted with **2** for 1 h prior to the addition of **3a**. [b] Estimated by GPC in THF on the basis of a linear polystyrene calibration. [c] Data taken from Table 1, entry. 4.

Table 4 Polymerization of **1**, **2** and **3**[a]

Entry	Monomer	Yield (%)	*Z*/*E*	M_w[b]	M_n[b]	M_w/M_n[b]
1[c]	**1** + **2** + **3a**	86	9/91	34 600	12 400	2.8
2	**1** + **2** + **3b**	91	15/85	32 100	14 000	2.3

[a] Carried out in THF under nitrogen at room temperature for 30 h in the presence of $Pd(PPh_3)_2Cl_2$, CuI and Et_3N. [Pd] = 4 mol%, [Cu] = 8 mol%, [Et_3N] = 0.1 M, [**1**] = 0.05 M, [**2**] = 0.05 M, [**3**] = 0.15 M. Monomer **1** reacted with **2** for 1 h prior to the addition of **3**. [b] Estimated by GPC in THF on the basis of a linear polystyrene calibration. [c] Data taken from Table 1, entry. 4.

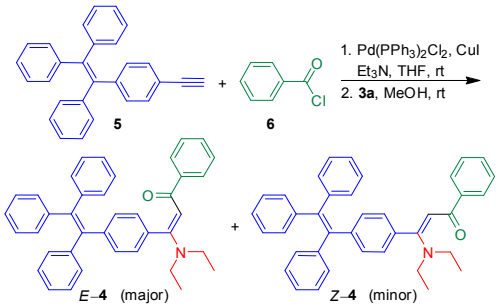

Scheme 3. Synthetic route to model compound **4**.

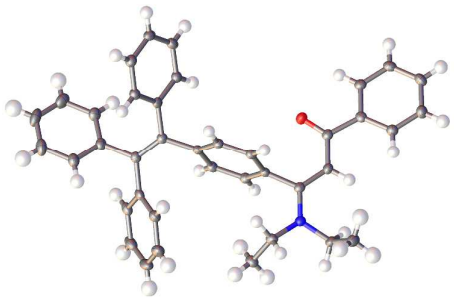

Fig. 1 ORTEP drawing of crystal structures of **4** (CCDC 1009269).

Structural Characterization

To confirm the occurrence of the sequential coupling-hydroamination polymerization and assist the characterization of the polymer structure, model reaction was performed (Scheme 3). Under the same conditions for preparing the polymers, the coupling reaction of monoyne **5**[16] and commercially available benzoyl chloride **6** followed by hydroamination of the intermediate with **3a** generated a isomeric mixture of model compound **4** (Scheme 3). Single crystals were obtained from their dichloromethane/hexane solution and three crystals were randomly chosen for single-crystal X-ray diffraction. All of them showed the same crystal structure (Fig. 1). Detailed crystal data were summarized and given in Table S1. Through such analysis, it was recognized that the major product generated during the one-pot sequential reaction was the *E*-isomer. Together with the data from NMR analysis, the sequential coupling-hydroamination reaction was proved to proceed regioselectively and stereoselectively, giving exclusive addition product with high *E*-content of up to 93%.

The chemical structures of model compound **4** and corresponding polymers (P**1**/**2**/**3**) are fully characterized by standard spectroscopic techniques with satisfactory results. The IR and NMR spectra of P**1**/**2**/**3a**, its monomers (**1**, **2** and **3a**) and model compound **4** are shown as examples. The two absorption bands observed at 2106 and 3275 cm^{-1} in monomer **1** were associated with its C≡C and ≡C–H stretching vibrations, respectively (Fig. 2). All these bands disappeared in the spectra of **4** and P**1**/**2**/**3a**, demonstrating the complete consumption of the C≡C functionality by model reaction and polymerization. Meanwhile, the carbonyl stretching vibration of **2** absorbed at

1726 cm^{-1}, which shifted to 1626 cm^{-1} after the sequential reaction.

The ^{1}H and ^{13}C NMR spectra provide detailed information on the structures of model compound and the polymers. As shown in Fig. 3, the resonance of the ethynyl protons of monomer **1** peaked at δ 3.03, which entirely disappeared in the spectra of **4** and P**1**/**2**/**3a**. After hydroamination, the resonance of the CH_2 protons next to the nitrogen atom of **3a** at δ 2.63 shifted to low field at δ ~3.37. In contrast, the absorption of the aromatic protons of **2** at δ 8.25 moved to high field. On the other hand, new peaks assigned to resonances of the newly formed C=CH functionality emerged in the spectra of **4** and P**1**/**2**/**3a**. Due to different chemical environments, the *E*- and *Z*-olefin protons could be readily distinguished in the spectra of **4** and P**1**/**2**/**3a**. While the *E*-olefin proton absorbed at δ 5.87, its *Z*-counterpart resonated at δ 5.67. Meanwhile, the *Z*- and *E*-isomers could be also differentiated from the absorptions of the aromatic protons adjacent to the carbonyl group at δ 7.97 (*Z*-**4**) and 7.84 (*E*-**4**). From the peak integrals at δ 5.87 and 5.67, the *E*/*Z*-olefin ratios of **4**, P**1**/**2**/**3a** and P**1**/**2**/**3b** were calculated to be 93/7, 91/9 and 85/15, respectively, indicating high stereoselectivity of the hydroamination reaction.

Similarly, the spectra of **4** and P**1**/**2**/**3a** showed no resonances of the acetylene carbons of **1** at δ 77.7 and δ 83.9 (Fig. 4). Instead, a new peak associated with the resonance of the newly formed olefin carbon (=*C*Ar(NR_2)) was observed at δ 163.3. This demonstrates that the acetylene group of **1** was completely transformed into olefin unit. On the other hand, the carbonyl carbon resonance of **2** was observed at δ 167.7, which downfield shifted to δ 187.2 after the polymerization. In addition, two peaks, owing to the absorptions of *E*- and *Z*-olefin carbons in =*C*H(COAr) fractions, emerged at δ 93.8 and 99.2 in the spectrum of **4.** All the obtained results were well consistent with those from the ^{1}H NMR analysis, proving the occurrence of the sequential coupling-hydroamination reaction. P**1**/**2**/**3a** shared similar NMR spectral patterns with **4**, confirming desired molecular structure as shown in Scheme 2.

Solubility and Thermal Stability

The resulting conjugated polymers can be readily soluble in common organic solvents, such as dichloromethane, chloroform, THF, DMF, etc., though they are comprised of many aromatic rings. It is largely attributed to the twisted TPE units in the polymer backbone. Furthermore, they possess good film-forming ability and uniform tough solid films can be readily obtained by spin-coating their solutions. The thermal stability of the polymers was then evaluated by thermogravimetric analysis (TGA). As shown in Fig. S1, P**1**/**2**/**3** lose 5% of their weights at 297–313 °C under nitrogen, revealing their reasonably high resistance to thermolysis at high temperature.

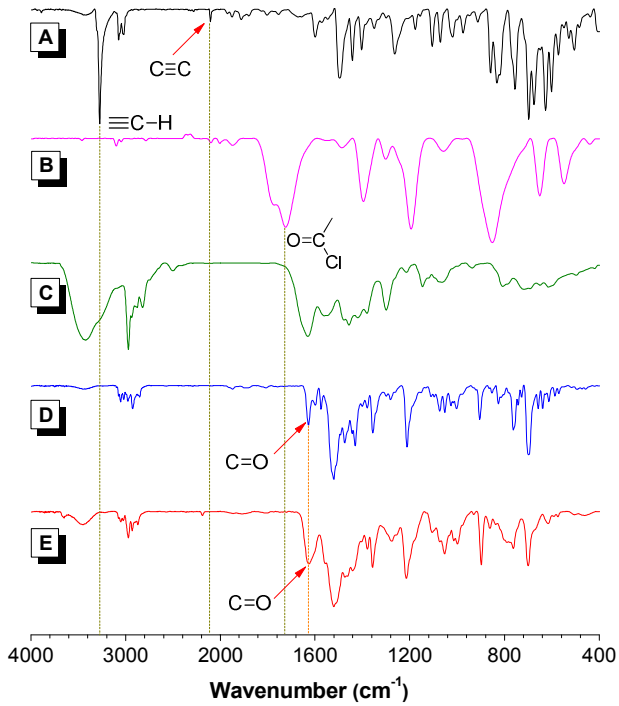

Fig. 2 IR spectra of (A) **1**, (B) **2**, (C) **3a**, (D) **4** and (E) P**1**/**2**/**3a**.

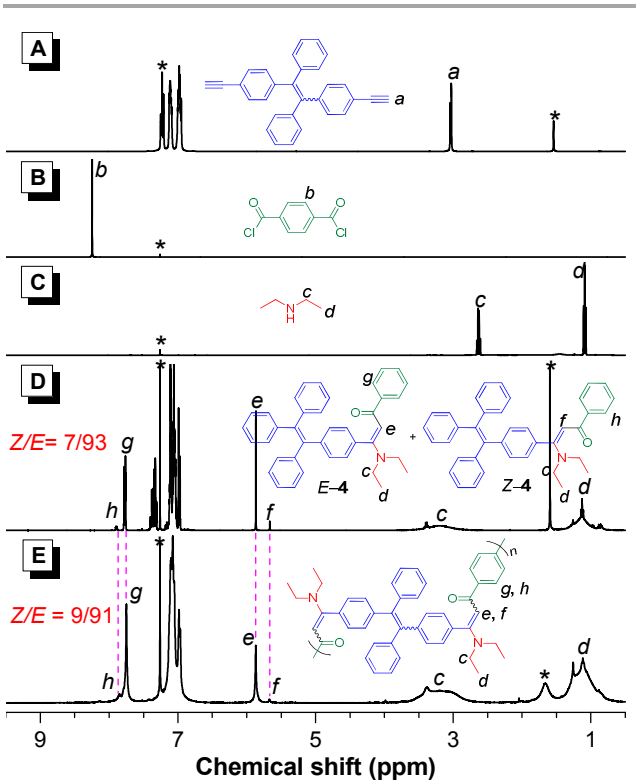

Fig. 3 ^{1}H NMR spectra of (A) **1**, (B) **2**, (C) **3a**, (D) **4** and (E) P**1**/**2**/**3a** in $CDCl_3$.

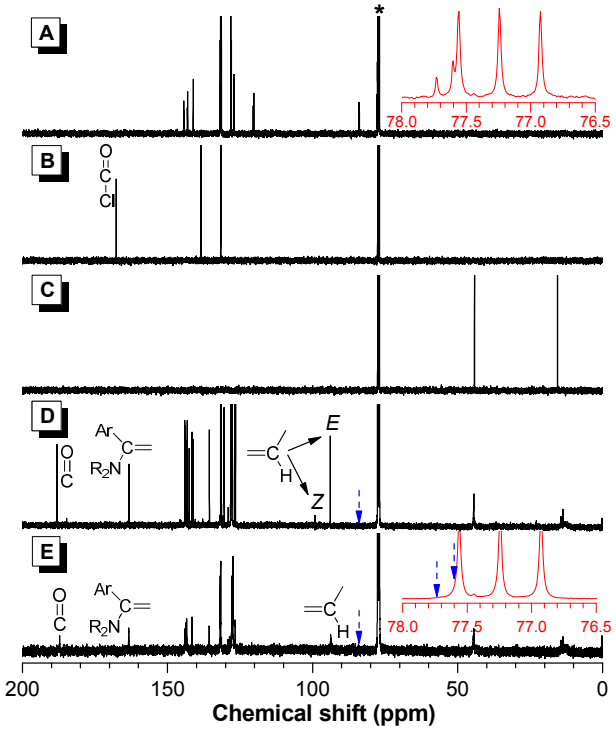

Fig. 4 ^{13}C NMR spectra of (A) **1**, (B) **2**, (C) **3a**, (D) **4** and (E) P**1**/**2**/**3a** in $CDCl_3$.

Light Refractivity and Chromatic Dispersion

Processable macromolecules with high refractive indices (*n* or RI) are promising materials with a variety of practical applications, such as in advanced optoelectronic fabrications of lenses, prisms, memories, substrates for advanced display devices, etc.[17] Conventional organic polymeric materials, including polycarbonate, poly(methyl methacrylate) and polystyrene, exhibit low refractive indices in the range of 1.49–1.58,[18] which limits their photonic applications. Conjugated polymers P**1**/**2**/**3** are comprised of abundant polarizable aromatic rings, TPE moieties, carbonyl groups, heteroatoms and a conjugated polymer backbone. Thus they are expected to exhibit high *n* values. This is proved to be the case. As shown in Fig. 5A, the thin films of P**1**/**2**/**3a** and P**1**/**2**/**3b** exhibited high *n* values of 1.9318–1.6413 and 1.8445–1.6320 in a wide wavelength region of 400–1000 nm, respectively.

It is also of great importance to develop polymeric materials with tunable refractive indices,[19] as the modulation of refractive index is a critical technological issue in optical communication and optical data storage devices.[20] Since the carbonyl groups and the vinyl units in P**1**/**2**/**3** are photosensitive,[21] their structures and hence their n values may be readily changed by light irradiation. Indeed, when a thin film of P**1**/**2**/**3a** was exposed to UV light for 20 min, its *n* values dropped rapidly to 1.6977–1.5918 in the wavelength range of 400–1000 nm. This indicates the efficient RI tunability of the polymer.

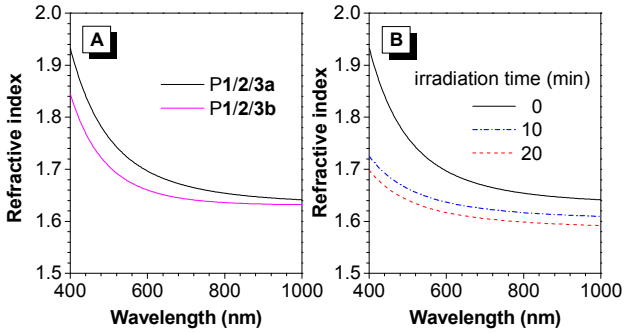

Fig. 5 (A) Wavelength dependence of refractive indices of thin films of P**1**/**2**/**3**. (B) Change in refractive index of a thin film of P**1**/**2**/**3a** by UV irradiation.

Table 5. Refractive indices and chromatic dispersions of P**1**/**2**/**3** before and after UV irradiation[a]

No.	Polymer	Time (min)	$n_{632.8}$	ν_D	D
1	P**1**/**2**/**3a**	0	1.6847	7.2259	0.1384
2	P**1**/**2**/**3a**	10	1.6316	16.9677	0.0589
3	P**1**/**2**/**3a**	20	1.6122	16.9783	0.0589
4	P**1**/**2**/**3b**	0	1.6526	9.7128	0.1030

[a]Abbreviation: n = refractive index, ν_D = Abbé number = $(n_D-1)/(n_F-n_C)$, where n_D, n_F and n_C are the n values at wavelengths of 589.2, 486.1 and 656.3 nm, respectively, D = chromatic dispersion = $1/\nu_D$

The Abbé number (ν_D) of a material describes the variation or dispersion in its *n* values with wavelength. Normally a small ν_D value may lead to undesired effect on the images' resolution. Polymers with high ν_D values or low chromatic dispersions D ($D = 1/\nu_D$) are promising candidates in a wide range of applications. The equation for calculating ν_D is: $\nu_D = (n_D - 1)/(n_F - n_C)$, where n_D, n_F and n_C are the n values at wavelengths of 589.3, 486.1 and 656.3 nm, respectively. As shown in Table 5, P**1**/**2**/**3a** and P**1**/**2**/**3b** possessed similar ν_D and D values. On the other hand, the ν_D values of P**1**/**2**/**3a** after UV treatment fell in the range of 7.2259–16.9783, corresponding to D values of 0.1384–0.0589. Hence, the RI tunability and low optical dispersion of the present polymers allow them to be promising coating materials in the advanced optical display systems.[22]

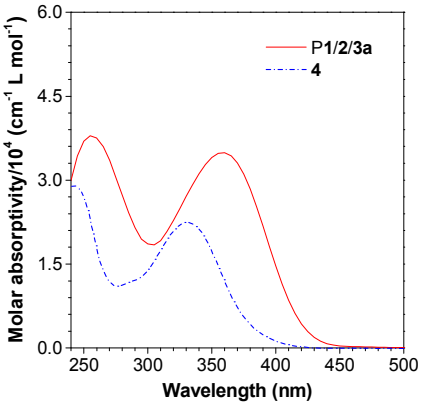

Fig. 6 Absorption spectra of **4** and P**1**/**2**/**3a** in pure THF solutions. Solution concentration: 10 μM.

Photophysical properties

Fig. 6 shows the UV spectra of **4** and P**1**/**2**/**3a** in diluted THF solutions (10 μM). The absorption maximum of **4** peaked at 330 nm, whilst, that of P**1**/**2**/**3a** was located at 360 nm, indicating a better conjugation in the polymer. On the other hand, TPE and its derivatives are well-known fluorophores with AIE characteristics.[23] The restriction of intramolecular rotation (RIR) process was proposed as the main cause for their AIE effect.[24] In solution, the phenyl rings rotate via the single-bond axes, serving as a relaxation channel for the decay of excited states and hence rendering the molecules nonemissive. In the aggregated state, such rotation is physically restricted, which blocks the nonradiative decay pathway and thus allows the molecules to emit intensely. As expected, **4** and P**1**/**2**/**3a** were non-emissive in THF (Fig. S2 and S3). Surprisingly, no signals were recorded even they were aggregated upon the addition of a large amount of poor solvent (water) into their THF solutions.

What is the cause for this phenomenon? Careful investigation of their molecular structures reveals that the PET process from the amine moiety to the excited fluorophore unit should be responsible for such behavior. If the amine group is protonated, the PET process may be forbidden and the emission of the polymer may be recovered. To prove this, we studied the emission property of P**1**/**2**/**3a** again in THF/water mixtures acidified with 1 mM of hydrochloric acid (Fig. 7). In pure THF solution, weak emission band with maximum at 536 nm was detected. The emission decreased slightly when a small amount of water content (≤30 vol %) was added to the THF solution, presumably due to the enhancement of the intramolecular charge transfer effect from the electron-donating amine unit to the electron-accepting carbonyl group. Afterwards, the intensity increased gradually without a noticeable emission peak shift due to the activation of the RIR process by aggregate formation. The highest emission intensity was achieved in THF/water mixture at 90% water fraction, which was about 4.0-fold higher than that in pure THF solution. The fluorescent photographs of P**1**/**2**/**3a** in THF and 95% aqueous solution taken under UV irradiation were shown in the inset of Fig. 7B. Compared to the weak emission in THF solution, the aggregates of P**1**/**2**/**3a** formed in THF/water mixture were more emissive. Clearly, aggregates formation has enhanced the emission of P**1**/**2**/**3a**. A similar phenomenon was also observed when a lower concentration of hydrochloride acid (0.5 mM) was used (Fig. S4).

To illustrate the PET process, the frontier orbital theory was present in Fig. 8A. Generally, a typical PET system comprises an aliphatic amine, a fluorophore and a short methylene chain as the linker. When excited by an appropriate light, the electron in the highest occupied molecular orbital (HOMO) of the fluorophore was promoted to the lowest unoccupied molecular orbital (LUMO). As the HOMO of an aliphatic amine was located between the LUMO and HOMO of the fluorophore, the amine electron could easily transfer to the HOMO of the fluorophore. This hinders the return of electron in the LUMO to the HOMO, thus leading to the emission quenching. When the amine groups were protonated, its HOMO was then located at the lower enegy than the HOMO of the fluorophore (Fig. 8B). This makes the PET process difficult to occur. Now, the electron in the LUMO of the fluorophore could undergo radiative decay, which recovered the emission of the polymer.

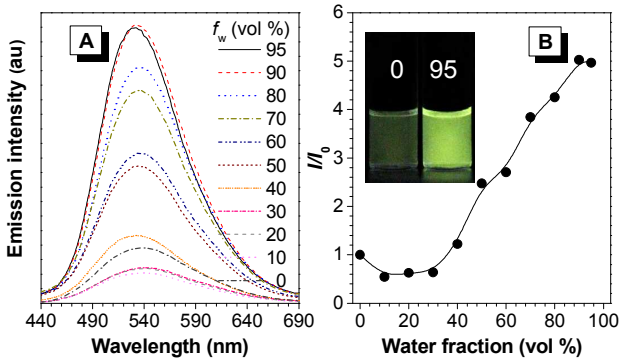

Fig. 7 (A) Emission spectra of P**1**/**2**/**3a** in THF/water mixtures with different water fractions (f_w) acidified with 1 mM of hydrochloric acid. (B) Plot of relative emission intensity (I/I_0) versus the composition of the acidified aqueous solution of P**1**/**2**/**3a**. Inset: Fluorescent photographs of P**1**/**2**/**3a** in THF/water mixtures with f_w of 0% and 95% taken under UV light irradiation. Solution concentration: 10 μM; excitation wavelength: 360 nm.

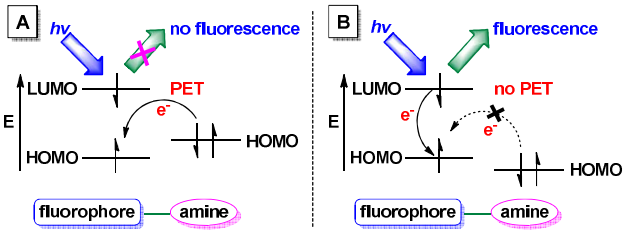

Fig. 8 Frontier molecular orbital theory of the PET process.

Conclusions

In this work, we developed an efficient one-pot multicomponent sequential polymerization approach to access functional polymers. The coupling-hydroamination polymerization of diyne, diaroyl chloride and secondary amine was catalyzed by $Pd(PPh_3)_2Cl_2$ and CuI in regio- and stereoselective manners, affording conjugated heteroatom-substituted polymers with high molecular weights in satisfactory yields. All the polymers were soluble, showing good film-forming ability and reasonably high thermal stability. They exhibited high tunable refractive indices in a wide wavelength region. They were weakly emissive in both solution and aggregated states due to the PET effect, although they possessed the TPE chromophoric unit. Their strong aggregated-state emission, however, could be readily recovered by protonation. Thus, the present work paves a way to facile synthesis of heteroatom-containing polymers with stimuli-responsive properties.

Experimental

Materials

THF was distilled from sodium benzophenone ketyl under nitrogen and then used immediately. Terephthaloyl dichloride and Et_3N were purchased from Sigma-Aldrich. $Pd(PPh_3)_2Cl_2$, CuI and methanol were ordered from Zhejiang Metallurgical Research Institute Co., Ltd., International Laboratory USA, and Merck, respectively. Other chemicals and reagents were all

purchased from J&K or Aldrich. All of the chemicals and solvents were used as received without further purification. Diyne **1** and monoyne **5** were synthesized according to procedures reported in the literatures.[16]

Instrument

The ^{1}H and ^{13}C NMR spectra were recorded on a Bruker ARX 400 NMR spectrometer using $CDCl_3$ as solvent and tetramethylsilane (TMS; δ = 0 ppm) as internal standard. High resolution mass spectra (HRMS) and IR spectra were collected on a GCT Premier CAB 048 mass spectrometer operated in MALDI-TOF mode and a PerkinElmer 16 PC FT-IR spectrophotometer, respectively. Single crystal X-ray diffraction was carried out at 100 K on a Bruker-Nonius Smart Apex CCD diffractometer with graphite monochromated Mo-Kα radiation. Analysis of the data was acquired through the SAINT and SADABS routines, meanwhile, the structure and refinement were obtained from the SHELTL suite of X-ray programs (Version 6.10). The weight-average molecular weights (M_w) and number-average molecular weights (M_n) as well as the polydispersity indices (M_w/M_n) of the polymers were evaluated through a GPC system (Waters) equipped with UV, RI and fluorescence detectors. THF (HPLC grade) was used as eluent at a flow rate of 1.0 mL min^{-1}. A series of standard linear polystyrenes covering the molecular weight range of 10^3–10^7 were employed for the molecular weight calibration. The polymeric products were dissolved in THF (~2 mg mL^{-1}), filtered through 0.45 μm PTFE syringe-type filters and injected into the GPC system for measurements afterwards.

A PerkinElmer TGA 7 analyzer was employed to estimate TGA thermograms under nitrogen at a heating rate of 10 $^{\circ}$C min^{-1}. The UV-vis absorption spectra, emission spectra and *n* values were measured on a Milton Roy Spectronic 3000 array spectrophotometer, a PerkinElmer LS 55 spectrofluorometer and a J. A. Woollam M-2000V multiwavelength ellipsometer, respectively. The polymer films were prepared by spin-coating the polymer solutions (10 mg in 1 mL of 1,2-dichloroethane) at 1000 rpm for 1 min on silicon wafers and then dried in a vacuum oven at room temperature overnight. Modulation of the RI values of the polymer films was achieved by UV irradiation from a Spectroline ENF-280C/FUV lamp with intensity of *ca.* 18.5 mW cm^{-2} at a distance of 3 cm.

Polymer Synthesis

All the polymerization reactions were carried out under nitrogen using a standard Schlenk technique. A typical polymerization procedure of **1**, **2** and **3** was given below as an example.

Into a 25 mL Schlenk tube equipped with a magnetic stirrer were charged diyne **1** (0.2 mmol, 76.1 mg) and terephthaloyl chloride **2** (0.2 mmol, 40.6 mg). Then, $Pd(PPh_3)_2Cl_2$ (0.008 mmol, 6.0 mg), CuI (0.016 mmol, 3.0 mg), 4.0 mL of THF and 0.06 mL of Et_3N were subsequently added under nitrogen. After reacting for 1 h at room temperature, diethylamine **3a** (0.6 mmol, 0.06 mL) and 0.5 mL of methanol ($V_{methanol}$: V_{THF} = 1:8) were injected into the reaction system. The mixture was further reacted for 30 h at the same temperature under nitrogen. Afterwards, the solution was added dropwise into 300 mL of methanol under stirring through a cotton filter. The formed precipitates were collected by filtration, washed with methanol and further dried under vacuum at room temperature to a constant weight.

P**1**/**2**/**3a** (Table 4, entry 1): Yellow powder; yield 86%. M_w = 34 600; M_w/M_n = 2.8. IR (KBr), υ (cm^{-1}): 3061, 3028, 2923, 2884, 2832, 2807, 1662, 1603, 1494, 1453, 1281, 1219. ^{1}H NMR (400 MHz, $CDCl_3$), δ (TMS, ppm): 7.85, 7.75, 7.11, 7.10, 7.08, 7.06, 6.99, 6.97, 5.87, 5.67, 3.38, 1.26. ^{13}C NMR (100 MHz, $CDCl_3$), δ ($CDCl_3$, ppm): 187.23, 163.35, 143.93, 143.63, 143.27, 141.59, 135.62, 131.84, 131.67, 127.82, 127.54, 127.40, 126.69, 93.75, 44.48, 13.62.

P**1**/**2**/**3b** (Table 4, entry 2): Yellow powder; yield 91%. M_w = 32 100; M_w/M_n = 2.3. IR (KBr), υ (cm^{-1}): 3061, 3025, 2953, 2830, 2805, 1664, 1594, 1494, 1453, 1280, 1218. ^{1}H NMR (300 MHz, $CDCl_3$), δ (TMS, ppm): 7.84, 7.73, 7.26, 7.09, 7.00, 6.96, 5.81, 5.66, 3.30, 2.88, 1.30, 0.95, 0.87 0.79. ^{13}C NMR (100 MHz, $CDCl_3$), δ ($CDCl_3$, ppm): 187.23, 163.35, 143.93, 143.63, 143.27, 141.59, 135.62, 131.84, 131.67, 127.82, 127.54, 127.40, 126.69, 93.75, 44.48, 32.70, 20.11, 13.62.

Model Reaction

Model compound 3-(diethylamino)-1-phenyl-3-(4-(1,2,2-triphenylvinyl)phenyl)prop-2-en-1-one (**4**) was synthesized according to a similar procedure for preparing P**1**/**2**/**3a** with some modifications.

Into a 25 mL Schlenk tube were placed monoyne **5** (0.5 mmol, 178.2 mg) and benzoyl chloride **6** (0.5 mmol, 0.06 mL). Then, $Pd(PPh_3)_2Cl_2$ (0.01 mmol, 8.0 mg) and CuI (0.02 mmol, 4.0 mg), 5.0 mL of freshly distilled THF and 0.06 mL of Et_3N were then added into the reaction system under nitrogen. After stirring at room temperature for 1 h, 1.0 mL of methanol and diethylamine **3a** (0.68 mmol, 0.07 mL) were injected. The mixture was allowed to react at room temperature for 18 h. The mixture was then extracted with 40 mL of water and 60 mL of dichloromethane three times. The organic layer was combined and dried over $MgSO_4$. The crude product was condensed and purified by silica-gel column chromatography using hexane/dichloromethane mixture (v/v = 5/1) as eluent. A white solid was obtained in 63% yield. IR (KBr), υ (cm^{-1}): 3061, 3025, 2972, 2916, 2845, 1626, 1524, 1477, 1427, 1352, 1207. ^{1}H NMR (400 MHz, $CDCl_3$), δ (TMS, ppm): 7.90 (d, 0.14 H), 7.77 (d, 1.86 H), 7.36 (m, 3 H), 7.13 (m, 17 H), 6.98 (d, 2 H), 5.87 (s, 0.93 H), 5.67(s, 0.07 H), 3.39 (q, 4 H), 1.13 (t, 6 H). ^{13}C NMR (100 MHz, $CDCl_3$), δ ($CDCl_3$, ppm): 188.11, 184.81, 163.26, 144.10, 143.81, 143.72, 143.17, 142.56, 141.49, 141.21, 135.55, 131.69, 131.67, 131.59, 131.55, 130.47, 128.05, 127.92, 127.86, 127.79, 127.68, 127.60, 126.70, 126.67, 126.58, 99.13, 93.88, 44.40, 13.66. HRMS (MALDI-TOF): *m/z* 534.2813 ([M+H]$^+$, calcd. 534.2791).

Preparation of aggregates

Stock THF solutions of **4** and P**1**/**2**/**3a** with a concentration of 1.0 mM were firstly prepared, respectively. Quantitative hydrochloric acid was added into the stock THF solution of P**1**/**2**/**3a** to afford an acidified one. Then 0.1 mL of stock THF solution of **4**, THF solution of P**1**/**2**/**3a** and acidified THF solution of P**1**/**2**/**3a** were transferred to 10.0 mL volumetric flasks, respectively. After addition of appropriate amounts of THF, water was added dropwise under vigorous stirring to furnish 1 × 10^{-5} M solutions with specific f_w of 0–95%. The absorption and emission spectra of the resulting solutions were then performed.

Acknowledgements

This work has been partially supported by National Basic Research Program of China (973 Program; 2013CB834701), the University Grants Committee of Hong Kong (AoE/P-03/08), the National Science Foundation of China (21490570 and 21490574), the Research Grants Council of Hong Kong (604913, 16305014 and 16303815), Science and Technology Plan of Shenzhen (JCYJ20140425170011516) and Natural Science Fund of Guangdong Province (2014A030313659). B. Z. Tang thanks the support of the Guangdong Innovative Research Team Program (201101C0105067115).

Notes and references

1 (a) S. E. Denmark and A. Thorarensen, *Chem. Rev.*, 1996, **96**, 137–165; (b) S. F. Mayer, W. Kroutil and F. Kurt, *Chem. Soc. Rev.*, 2001, **30**, 332–339; (c) H. Pellissier, *Chem. Rev.*, 2013, **113**, 442–524; (d) A. Behr, A. J. Vorholt, K. A. Ostrowski and T. Seidensticker, *Green Chem.*, 2014, **16**, 982–1006.

2 X. Zeng, *Chem. Rev.*, 2013, **113**, 6864–6900.

3 (a) R. R. Hu, J. W. Y. Lam and B. Z. Tang, *Macromol. Chem. Phys.*, 2013, **214**, 175–187; (b) J. W. Y. Lam and B. Z. Tang, *Acc. Chem. Res.*, 2005, **38**, 745–754.

4 (a) C. M. Marson, *Chem. Soc. Rev.*, 2012, **41**, 7712–7722; (b) L. Albrecht, H. Jiang and K. A. Jorgensen, *Angew Chem. Int. Edit.*, 2011, **50**, 8492–8509.

5 (a) J. L. Tucker, *Org. Process Res. Dev.*, 2006, **10**, 315–319; (b) I. T. Horvath and P. T. Anastas, *Chem. Rev.*, 2007, **107**, 2169–2173.

6 (a) S. M. Brombosz, S. Seifert and M. A. Firestone, *Polymer*, 2014, **55**, 3370–3377; (b) N. A. Rahim, F. Audouin, B. Twamley, J. G. Vos and A. Heise, *Eur. Polym. J.*, 2012, **48**, 990–996; (c) J. J. Haven, C. Guerrero-Sanchez, D. J. Keddie, G. Moad, S. H. Thang and U. S. Schubert, *Polym. Chem.*, 2014, **5**, 5236–5246; (d) Z. Q. Wu, Y. Chen, Y. Wang, X. Y. He, Y. S. Ding and N. Liu, *Chem. Commun.*, 2013, **49**, 8069–8071.

7 (a) A. J. Yang, R. W. Jiang, O. Khorev, T. Yu, Y. L. Zhang, L. P. Ma, G. H. Chen, J. K. Shen and T. Meng, *Adv. Synth. Catal.*, 2013, **355**, 1984–1988; (b) V. Gembus, J. F. Bonfanti, O. Querolle, P. Jubault, V. Levacher and C. Hoarau, *Org. Lett.*, 2012, **14**, 6012–6015; (c) S. G. Zhu, L. L. Wu and X. Huang, *RSC Adv.*, 2012, **2**, 132–134; (d) Z. J. Liu and R. C. Larock, *Angew Chem. Int. Edit.*, 2007, **46**, 2535–2538; (e) S. Pache and M. Lautens, *Org. Lett.*, 2003, **5**, 4827–4830.

8 C. Zheng, H. Q. Deng, Z. J. Zhao, A. J. Qin, R. R. Hu and B. Z. Tang, *Macromolecules*, 2015, **48**, 1941–1951.

9 H. Deng, R. Hu, E. Zhao, C. Y. K. Chan, J. W. Y. Lam and B. Z. Tang, *Macromolecules*, 2014, **47**, 4920–4929.

10 H. Deng, R. Hu, A. C. S. Leung, E. Zhao, J. W. Y. Lam and B. Z. Tang, *Polym. Chem.*, 2015, **6**, 4436–4446.

11 (a) A. S. Karpov and T. J. J. Müller, *Synthesis*, 2003, 2815–2826; (b) A. S. Karpov and T. J. J. Müller, *Org. Lett.*, 2003, **5**, 3451–3454.

12 (a) F. Pohlki and S. Doye, *Chem. Soc. Rev.*, 2003, **32**, 104–114; (b) T. E. Müller, K. C. Hultzsch, M. Yus, F. Foubelo and M. Tada, *Chem. Rev.*, 2008, **108**, 3795–3892; (c) R. Severin and S. Doye, *Chem. Soc. Rev.*, 2007, **36**, 1407–1420.

13 (a) J. Z. Liu, J. W. Y. Lam and B. Z. Tang, *Chem. Rev.*, 2009, **109**, 5799–5867. (b) A. J. Qin, J. W. Y. Lam and B. Z. Tang, *Chem. Soc. Rev.*, 2010, **39**, 2522–2544.

14 R. Hu, N. L. Leung and B. Z. Tang, *Chem. Soc. Rev.*, 2014, **43**, 4494–4562.

15 (a) D. T. McQuade, A. E. Pullen and T. M. Swager, *Chem. Rev.*, 2000, **100**, 2537–2574; (b) C. Wang, H. Dong, W. Hu, Y. Liu and D. Zhu, *Chem. Rev.*, 2012, **112**, 2208–2267.

16 R. Hu, J. L. Maldonado, M. Rodriguez, C. Deng, C. K. W. Jim, J. W. Y. Lam, M. M. F. Yuen, G. Ramos-Ortiz and B. Z. Tang, *J. Mater. Chem.*, 2012, **22**, 232–240.

17 (a) J. Liu and M. Ueda, *J. Mater. Chem.*, 2009, **19**, 8907–8919; (b) D. R. Robello, *J. Appl. Polym. Sci.*, 2013, **127**, 96–103; (c) T. Nakamura, H. Fujii, N. Juni and N. Tsutsumi, *Opt. Rev.*, 2006, **13**, 104–110.

18 (a) J. Brandrup, E. H. Immergut and E. A. Grulke, *Polymer handbook*, Wiley, New York, Chichester, 4th edn, 2004; (b) J. E. Mark, *Polymer data handbook*, Oxford University Press, Oxford, New York, 2009.

19 C. K. W. Jim, J. W. Y. Lam, A. J. Qin, Z. J. Zhao, J. Z. Liu, Y. N. Hong and B. Z. Tang, *Macromol. Rapid Commun.*, 2012, **33**, 568–572.

20 (a) T. Griesser, T. Höfler, G. Jakopic, M. Belzik, W. Kern and G. Trimmel, *J. Mater. Chem.*, 2009, **19**, 4557–4565; (b) M. Edler, S. Mayrbrugger, A. Fian, G. Trimmel, S. Radl, W. Kern and T. Griesser, *J. Mater. Chem. C*, 2013, **1**, 3931–3938.

21 P. S. Johnson, P. L. Cook, X. Liu, W. Yang, Y. Bai, N. L. Abbott and F. J. Himpsel, *J. Chem. Phys.*, 2011, **135**, 044702.

22 J. L. Regolini, D. Benoit and P. Morin, *Microelectron. Reliab.*, 2007, **47**, 739–742.

23 (a) Y. N. Hong, J. W. Y. Lam and B. Z. Tang, *Chem. Commun.*, 2009, 4332–4353; (b) Y. N. Hong, J. W. Y. Lam and B. Z. Tang, *Chem. Soc. Rev.*, 2011, **40**, 5361–5388.

24 J. Mei, Y. Hong, J. W. Lam, A. Qin, Y. Tang and B. Z. Tang, *Adv. Mater.*, 2014, **26**, 5429–5479.

25 (a) W. Zhang, Z. Ma, L. Du and M. Li, *Analyst*, 2014, **139**, 2641–2649; (b) A. P. de Silva, T. S. Moody and G. D. Wright, *Analyst*, 2009, **134**, 2385–2393.

Table of Contents Entry

Sequential coupling-hydroamination polymerization towards stimuli-responsive polymers